Engineering Applications of Computational Fluid Mechanics Vol. 3, No. 1, pp. 42–55 (2009)

STUDY OF RELATIVE ROLES OF NONLINEARITY AND DEPTH REFRACTION IN WAVE SPECTRUM EVOLUTION IN SHALLOW WATER

Vladislav G. Polnikov* and Sauro Manenti**

** A.M. Obukhov Institute for Atmospheric Physics, Pyzhevskii lane 6, Moscow, 119017 Russia*
*** Dipartimento di Idraulica Trasporti e Strade, University of Rome "Sapienza", via Eudossiana, 18–00184 Rome, Italy*
E-Mail: sauro.manenti@uniroma1.it (*Corresponding Author*)

ABSTRACT: For modelling a series of depth profiles covering the relative depth parameter interval $2>k_p h>0.3$, evolution of two-dimensional gravity wave spectra is calculated in the frame of three-wave quasi-kinetic approximation derived by Zaslavskii and Polnikov (1988). The relative impact of refraction and nonlinearity on a change of two-dimensional spectra shape for gravity waves is estimated. It is shown that on the background of refraction impact on the spectrum shape, the three-wave nonlinearity results in a remarkable change of angular and frequency distribution for a wave energy spectrum. Herewith, in the spectral peak domain the nonlinearity reduces the value of the angular narrowness parameter by 20–30%, counteracting the refraction during the wave propagation into a shoal zone. In contrast to the high frequency domain of the spectrum, the angular narrowness parameter is increased due to the nonlinearity. For this reason, the nonlinearity can result in more than 10% change of wave energy in a shallow water zone with respect to the linear wave evolution case. These conclusions were checked by using the SWAN model under the same conditions. It was found that the SWAN model describes some of the main peculiarities of nonlinear waves in shallow water. Some recommendations were made to elaborate the three-wave nonlinear term in the source function of the SWAN model.

Keywords: shallow water waves, refraction, nonlinearity, three-wave quasi-kinetic approximation, wave spectrum, spectrum shape parameters

1. INTRODUCTION

There are a lot of papers devoted to the investigation of nonlinear wave dynamics in shallow water (for references, see earlier papers: Freilich, Elgar and Guza, 1990; Beji and Battjes, 1993; Eldeberky, 1996; Young, Verhagen and Khatri, 1996; present state is presented in Proceedings of 29th International Conference of coastal Engineering, 2004). Interest in this topic is stimulated by both the scientific and practical aspects of the problem. From a scientific point of view, for example, it is very important to find out the relative roles of different wave evolution mechanisms in water of finite depth. In particular, the question of the relative roles of depth refraction and nonlinearity is one of the interesting points in the description of wave propagation to a shallow water zone. Besides, the answer to this question is necessary for the justification of the kind of numerical model to be used in practice (linear or nonlinear).

The solution of the question posed is difficult for the reason that depth refraction is essential only in the case of shallow water, when the relative depth $k_p h$ is rather small, i.e. in the case when $k_p h < 1$ (here k_p is the spectral peak wave number, and h is the local depth). But just in this case, the applicability of the standard four-wave approximation for the nonlinear wave evolution description fails (Zaslavskii, Krasitskii and Gavrilin, 1995; Zakharov, 1998). Up to the recent years there was no justified approximation for the spectral description of the nonlinear wave evolution mechanism in the frame of kinetic equation in the shallow water case when $k_p h < 1$. This problem was solved by Zaslavskii and Polnikov (1998) and Polnikov (1998) by constructing a so-called three-wave quasi-kinetic approximation for the description of the nonlinear wave spectrum evolution in shallow water. Applicability of this approximation to solution of practical problems was proved by the comparison of certain problem calculations with some laboratory experiments (Piscopia et al., 2003). Thus, at present the problem posed can be solved.

In the present paper we consider the simplest cases of the two-dimensional wave spectrum evolution in the three-wave quasi-kinetic approximation for modelling a series of one-

Received: 8 May 2008; Revised: 30 Jun. 2008; Accepted: 28 Jul. 2008

dimensional depth profiles. The main point of our investigations is to estimate the relative roles of depth refraction and nonlinearity in the process of gravity wave spectrum formation during wave propagation into a shallow water zone. To our knowledge, this problem is considered in scientific literature for the first time.

This paper is laid out as follows. In Section 2, we discuss the pose of the problem and introduce the necessary definitions and formulas. Method of numerical study is given in Section 3. Section 4 is devoted to results and analysis. In Section 5, we check features of nonlinear three-wave term of the SWAN model in light of the results obtained before. Final conclusions are made in Section 6.

2. THE PROBLEM POSED

As it is well known, in shallow water the evolution of waves is accompanied by the following four processes: shoaling, refraction, nonlinear interaction among waves, and shallow-water breaking (hereafter this kind of breaking is called "surfing" in accordance with Freilich, Elgar and Guza (1990) and Eldeberky (1996)). The latter process is modified by the bottom friction, but it is not important in the case under consideration. All these processes are described in a spectral representation by the following model (Polnikov and Sychev, 1996):

$$\frac{\partial \Phi}{\partial t} + C_g \cos\theta \frac{\partial \Phi}{\partial x} + C_g \sin\theta \frac{\partial \Phi}{\partial y} + C_\theta \frac{\partial \Phi}{\partial \theta} = F(\Phi) \tag{1}$$

where:

$$\Phi(\sigma,\theta,x,t) \equiv N(\mathbf{k},x,t) = (4\pi^2 g/\sigma) S(\mathbf{k},x,t) = (4\pi^2 g/\sigma) C C_g S(\sigma,\theta,x,t)/\sigma \tag{2}$$

is the two-dimensional spatial wave action spectrum $N(\mathbf{k})$, represented via the energy frequency-angle spectrum $S(\sigma,\theta)$ in the frequency-angle space (σ,θ); g is the gravity acceleration, $C = \sigma/k$ and $\mathbf{C}_g = \mathbf{k}\partial\sigma/k\partial k$ is the phase and group velocity of the wave component with the frequency σ and wave vector $\mathbf{k}$, related by the dispersion relation $\sigma(\mathbf{k})$. C_θ is the velocity of the wave energy transfer in the angle space (refraction) (Polnikov and Sychev, 1996):

$$C_\theta \equiv \frac{\partial\theta}{\partial t} = \frac{\sigma}{\sinh(2kh)}\left[\sin\theta\frac{\partial h}{\partial x} - \cos\theta\frac{\partial h}{\partial y}\right]. \tag{3}$$

F(Φ) is the total source function of the model, which, in general, includes both the nonlinear evolution mechanism (NL) and the dissipation one (BR). Given the qualitative characteristics of our investigation, later in this paper we use representation of the source function in the form:

$$F = c_{NL}\, NL. \tag{4}$$

Thus, we do not take into account any dissipation mechanisms. Expression for the term NL is given below. The coefficient c_{NL} takes the value 0 or 1 depending on the problem posed: linear or nonlinear. The shallow water dissipation term ("surfing" term) is omitted especially with the aim to determine the role of the nonlinear mechanism only[1].

To specify the nonlinear term NL we use the three-wave quasi-kinetic approximation, a short description of which is as follows (Zaslavskii and Polnikov, 1998). Under the assumption that nonlinear wave-wave processes are realized for a certain interaction time, the nonlinear evolution of a gravity wave spectrum is governed by the three-wave quasi-resonant interactions. In this case, instead of the single kinetic equation, dynamics of the two-dimensional spatial wave action spectrum, $N(\mathbf{k})$, is described by the NL function governed by a system of two equations as follows. One of them is the typical evolution equation:

$$\begin{aligned} NL \equiv \frac{\partial N(\mathbf{k})}{\partial t} = 4\pi \int d\mathbf{k}_1 \int d\mathbf{k}_2 \\ \times \Big\{ V_1^2(\mathbf{k},\mathbf{k}_1,\mathbf{k}_2)\delta(\mathbf{k}-\mathbf{k}_1-\mathbf{k}_2)\delta_\beta(k,-k_1,-k_2)\left[N(\mathbf{k}_1)N(\mathbf{k}_2) - N(\mathbf{k})(N(\mathbf{k}_1)+N(\mathbf{k}_2))\right] \\ - 2V_1^2(\mathbf{k}_1,\mathbf{k},\mathbf{k}_2)\delta(\mathbf{k}_1-\mathbf{k}-\mathbf{k}_2)\delta_\beta(k_1,-k,-k_2)\left[N(\mathbf{k}_2)N(\mathbf{k}) - N(\mathbf{k}_1)(N(\mathbf{k}_2)+N(\mathbf{k}))\right]\Big\} \end{aligned} \tag{5}$$

where instead of classical exact delta-function for frequencies, $\delta(\sigma(k) \pm \sigma(k_1) \pm \sigma(k_2))$, usually used in a traditional theory for nonlinear waves, the spread delta function is introduced. It has the form

[1] As shown in the special study of Piscopia et al. (2003), the role of the surfing term is very important for a comparison with measurements. But in modelling our posed problem, this term is not needed yet.

$$\delta_\beta(k,\ \pm k_1,\ \pm k_2) = \frac{1}{\pi}\frac{\beta(\mathbf{k})}{(\sigma(k) \pm \sigma(k_1) \pm \sigma(k_2))^2 + \beta^2(\mathbf{k})}\ . \tag{6}$$

The reason for such replacement is provided by the fact that nonlinear interactions are realised in shallow water for a rather short time, and a typical transition to the infinite time of nonlinear interactions is not valid in this case (for details, see Zaslavskii and Polnikov, 1988; Piscopia et al, 2003). Note that for $\beta(\mathbf{k}) \to 0$, according to Eq. (6), we have the traditional representation of the evolution equation, as far as the spread delta-function is going to be the exact one.

The spread delta-function has a parameter of spreading, $\beta(\mathbf{k})$, which should be defined self-consistently from the dynamic equations. It was proposed in the original paper (Zaslavskii and Polnikov, 1988) that this parameter is governed by the separate equation of the form

$$\begin{aligned}\beta(\mathbf{k}) = 4\pi \int d\mathbf{k_1} \int d\mathbf{k_2} \\ \times \Big\{ V_1^2(\mathbf{k},\mathbf{k}_1,\mathbf{k}_2)\delta(\mathbf{k}-\mathbf{k}_1-\mathbf{k}_2)\delta_\beta(k,-k_1,-k_2)\big[N(\mathbf{k_1})+N(\mathbf{k_2})\big] \\ + 2V_1^2(\mathbf{k}_1,\mathbf{k},\mathbf{k}_2)\delta(\mathbf{k}-\mathbf{k}_1+\mathbf{k}_2)\delta_\beta(k_1,-k,-k_2)\big[N(\mathbf{k}_2)-N(\mathbf{k}_1)\big]\Big\}.\end{aligned} \tag{7}$$

The description of nonlinear evolution mechanism for wave spectrum in the frame of Eqs. (5)–(7) was called the quasi-kinetic approximation (Zaslavskii and Polnikov, 1998).

In Eqs. (5) and (7), functions $V_1(\ldots)$ are the standard matrix elements for the three-wave interactions, which depend on the local depth h. Their explicit representation is as follows:

$$V_1(\mathbf{k},\mathbf{k}_1,\mathbf{k}_2,h) = -V(-\mathbf{k},\mathbf{k}_1,\mathbf{k}_2,h) - V(-\mathbf{k},\mathbf{k}_2,\mathbf{k}_1,h) + V(\mathbf{k}_1,\mathbf{k}_2,\mathbf{k},h) \tag{8}$$

where:

$$V(\mathbf{k},\mathbf{k}_1,\mathbf{k}_2,h) = \frac{1}{8\pi}\left[\frac{g\sigma(k_2)}{2\sigma(k)\sigma(k_1)}\right]^{1/2}\Big[\mathbf{k}(h)\mathbf{k}_1(h) + \sigma^2(k)\sigma^2(k_1)/g^2\Big]. \tag{9}$$

In the case of finite depth water, the proper frequency, $\sigma(k)$, of the wave with a wave-vector $\mathbf{k}(h)$ is given by the dispersion relation of the form:

$$\sigma(k) = [\, g\,k \tanh(kh)\,]^{1/2}\ . \tag{10}$$

Integration used in Eqs. (5) and (7) is carried out through the whole **k**-space.

For the case of unidirectional waves, the quasi-kinetic approximation was studied in Zaslavskii and Polnikov (1998) and Polnikov (1998). Peculiarities of two-dimensional energy transfer through the wave spectrum were considered in Polnikov (2000). But spatial evolution of two-dimensional wave spectrum was not investigated in this approximation yet.

Thus, the problem is to solve Eq. (1) with the source function (4) in the approximations (5)–(7) for a series of modelling configurations of the depth profile and for several different kinds of the initial two-dimensional wave energy spectrum shape, $S(\sigma, \theta)$. The relative role of refraction and nonlinearity is defined by the analysis of the spectral shape parameters change for the linear and nonlinear problems posed for Eq. (1).

In particular, we pose a task to estimate the influence of nonlinearity (assuming that $k_p h < 1$) on the following spectral shape parameters:

a) the spatial wave energy distribution

$$E(x) = \int S(x,\sigma,\theta)\,d\sigma\,d\theta, \tag{11}$$

b) the frequency width of the spectrum

$$B(x) = E(x)/S_p(x)/\sigma_p(x), \tag{12}$$

c) the angular narrowness of the wave spectrum

$$A(\sigma;x) = S(\sigma,\theta_p;x)/S(\sigma;x). \tag{13}$$

Here σ_p, θ_p and $S_p = S(\sigma_p)$ are the frequency-angular coordinates of the spectral peak and the value of the latter, respectively. Sometimes we consider dependence of angular narrowness parameter at peak frequency σ_p on the space:

$$A(\sigma_p, x) = A_p(x). \tag{14}$$

The choice of the wave energy spectrum $S(\sigma, \theta)$ for analysis, instead of the wave action spectrum $N(\mathbf{k})$ is due to the fact that the energy spectrum is the most widely measured in situ, and the values of the shape parameters for this spectrum are well known.

3. METHOD OF INVESTIGATION

For a study of refraction effects on frequency-angular spectrum it needs to find a solution of Eq. (1) in two-dimensional space (x, y). A peculiarity of the quasi-kinetic approximation consists in a necessity to solve Eq. (7) with respect to $\beta(\mathbf{k})$ at each time step for each point of the spatial grid. Then, a value of the term NL is defined from Eq. (5), and Eq. (1) can be solved. As the matrix elements, $V_1(\ldots)$, depend on the local depth $h(x, y)$, the problem posed becomes rather complicated from a numerical point of view. But for simplified depth profiles $h(x, y)$, and with a proper choice for the frequency set $\{\sigma_k\}$ $(1 \le k \le K)$, angle set $\{\theta_m\}$ $(1 \le m \le M)$, and the spatial grid $\{x_i, y_j\}$ $(1 \le i \le I,\ 1 \le j \le J)$, the problem posed is executable by means of modern PC of moderate power.

It should be mentioned that the quasi-kinetic approximation has a certain theoretical restriction of applicability with respect to the time scale: a value of the spreading parameter $\beta(\mathbf{k})$ has to be smaller than the typical frequency $\sigma(k, h)$ of the waves under consideration (Zaslavskii and Polnikov, 1998). But in real calculations, applicability of the theory is tested by verification of the model as a whole for a certain geometry of a system under consideration. Proper estimations of applicability of the approximation were made in Piscopia et al. (2003) for a series of tank experiment data. On this basis, a choice of spatial scales of the basin under investigation was taken in accordance with experimental situations described in Beji and Battjes (1993) and Piscopia et al. (2003).

3.1 Depth profiles and boundary conditions

First of all, let us specify the depth profiles. To serve our aims, the case of isobaths parallel to the strait shoreline are quite acceptable. For the case of the x-axis directed normal to the shoreline, wave field parameter distributions can be described by one-dimensional arrays of the kind $P\{x_i\}$ $(1 \le i \le I)$ with the minimal value of y-points ($J = 3$) which are needed to secure the so-called "fluid" lateral boundary conditions. For such boundary conditions, at each time step, wave spectrum values at the lateral boundaries, $j = 1$ and $j = 3$, are equal to the ones calculated for the spectrum at the internal grid line, $j = 2$. Such an approach for the boundary conditions permits to minimize the number of pre-calculated matrix elements in Eq. (8) and the time of calculations.

In the case of constant depth slope, the depth profile can be given by the formula, which in a discrete representation has the form:

$$h(x_i) = h_0 - s\Delta x \cdot i. \qquad (15)$$

Here h_0 is the depth at the outer boundary (far from the shore), s is the value of slope, Δx is the spatial step normal to the shore, and i is the current number of the spatial point. In this case, the main calculations were executed under the following conditions: $h_0 = 5$ m, $s = 0.025$, $\Delta x = 20$ m, $I = 10$ (i.e. $5\ \text{m} \ge h(x) \ge 0.5$ m, see Fig. 1a). The value of Δy is not important, in the case of fluid boundaries (for certainty, we use $\Delta y = \Delta x$).

Together with the profile mentioned, it is interesting to consider the depth profile with a shallow water bar (Fig. 1b). Our experience (Piscopia et al., 2003) shows that a depth profile with a bar is rather informative, from the physical point of view. In our case of a shallow water bar, the depth profile is given by the following ratios (in meters):

$$h(1) = h(2) = h(3) = 2;$$
$$h(4) = 1.5;$$
$$h(5) = h(6) = 1;\ h(7) = 1;$$
$$h(8) = 1.5;$$
$$h(9) = h(10) = 2. \qquad (16)$$

The step of the spatial grid is the same: $\Delta x = 20$ m.

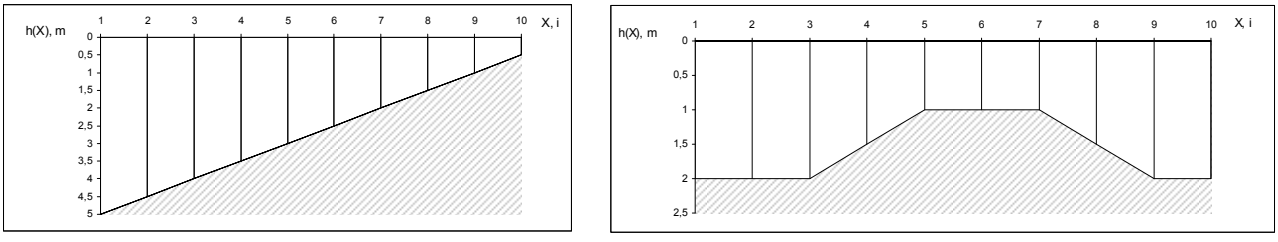

Fig. 1 A typical scheme of bottom profiles under consideration: a) with a constant slope, b) with a bar.

3.2 Frequency-angle set

Taking into account the depth profile features, the peak frequency, σ_p, and the frequency set, $\{\sigma_k\}$, are chosen to secure the following relative depth interval, $2 > k_p h > 0.3$. Herewith, the upper frequency value of the set $\{\sigma_k\}$ is to be more than $2.5\,\sigma_p$. The latter requirement is due to the fact that the three-wave interactions do form a local spectral maximum near the doubled peak frequency (Polnikov, 1998 & 2000). This process should be correctly described in numerical simulations. As a result, the set of cyclic frequencies (Hz) was given by the ratio:

$$f_k = 0.03 + 0.03\,(k-1), \quad (k = 1, 2, \ldots, 20) \qquad (17)$$

with the choice $f_p = 0.24$ Hz. (The angular frequencies, σ_k, are calculated by the ratio $\sigma_k = 2\pi f_k$).
The angle set was given by the ratio:

$$\theta_m = -\pi/2 + (m-1)\pi/18, \quad m = 1, 2, \ldots, 19 \qquad (18)$$

with the choice of general direction $\theta = 0$ corresponding to the normal of the shore.

3.3 Initial spectrum

The shape of initial energy spectrum is given in the *JONSWAP* form. Herewith, one should keep in mind that just the frequency σ_k is a constant parameter of the wave component propagating into shallow zone, whilst the wave number k is defined by the dispersion relation (10). As it was shown in Kitaigorodskii, Krasitskii, and Zaslavskii (1975), the spatial spectrum shape $S(\mathbf{k})$ does not depend upon the depth. Thus, for the correctness of calculations, the initial spectrum should be prescribed in the universal spatial representation $S(\mathbf{k})$ rather than in the frequency-angular one, i.e. $S(\sigma, \theta)$. So, for the initial spectrum in the *JONSWAP* one should use representation of the form:

$$S(\mathbf{k}) = S(k)\,\Psi(\theta)/k$$
$$= (\alpha/2)\,k^{-4} \exp\left[-2\,(k_p/k)^2\right] J(k_p/k)\,\Psi(\theta). \qquad (19)$$

Here α is the Phillips' constant (in our case $\alpha = 0.01$), $J(\ldots)$ is the non-dimensional peak enhancing function of the JONSWAP-type, introduced in Hasselmann et al. (1976) for more generality of the spectral shapes under consideration, and $\Psi(\theta)$ is the angular spreading function.
In this representation $J(\ldots)$ has the form:

$$J(k_p/k) = \gamma \exp\left[\frac{\left((k/k_p)^{1/2} - 1\right)^2}{2\Delta^2}\right] \qquad (20)$$

where the following values are used for the shape parameters: $\gamma = 1, 3$ and $\Delta = 0.1$. The angular spreading function is given by the formula:

$$\Psi(\theta) = Q(n)\cos^n\theta \qquad (21)$$

where $Q(n) = 1/\int \cos^n\theta\, d\theta$ is the normalizing coefficient. The typical set of the cosine power values is $n = 2$, 12. Transition from $S(\mathbf{k})$ to $S(\sigma, \theta)$ is governed by the formula:

$$S(\sigma, \theta) = S(\mathbf{k})\left[\frac{\sigma}{(\sigma/k)(\partial\sigma/\partial k)}\right]. \qquad (22)$$

Thus, from the very beginning, the frequency-angular set, $\{\sigma_k, \theta_m\}$, is given. Further it is recalculated into the set $\{k_k, \theta_m\}$ for the fixed local depth at each spatial grid point to define the initial spectrum given by Eq. (19). After executing the wave evolution calculation, analysis of the output spectral shape is done for the traditional representation of the spectrum, i.e. for $S(\sigma, \theta)$.

3.4 Numerical scheme for solution of Eq. (1)

Rather effective numerical scheme for solution of Eq. (1) was proposed earlier in Polnikov and Sychev (1996). The distinctive feature of this choice consists in the use of the upward implicit scheme of the first order for the advective terms of the model only, whereas for the refractive term the explicit scheme is used for numerical simplicity. As a result, to calculate the spectral component $\Phi(x_i, y_j, \sigma_k, \theta_m, t_n)$ at the $(n+1)$-th time step, for each frequency σ_k we have the following ratio:

$$\Phi^{n+1}_{ijm} = (F^n_{ijm} + \Delta t'\Phi^n_{ijm} + \Delta x'\Phi^{n+1}_{i-1jm} + \Delta y'\Phi^{n+1}_{ij-1m} + \Delta\theta'\Phi^n_{ijm-1})/(\Delta t' + \Delta x' + \Delta y' + \Delta\theta'). \qquad (23)$$

Here n, i, j, m are the indexes for the variables t, x, y, θ, respectively, with the proper steps, Δt, Δx, Δy and $\Delta\theta$; $F^n_{ijm} \equiv F(\Phi^n_{ijm})$ is the source function value at the proper point of calculations, and $\Delta t' = 1/\Delta t$, $\Delta x' = C_{gx}/\Delta x$, $\Delta y' = C_{gy}/\Delta y$, $\Delta\theta' = C\theta/\Delta\theta$. The experience of using scheme (23) has shown that it may be

applicable for both stationary and non-stationary descriptions of the wave field, with a rather quick convergence of the solution (Polnikov and Sychev,1996). Herewith, for the linear case, the stationary case is realized simply by putting $\Delta t \to \infty$ (or $\Delta t' \to 0$). But for the nonlinear case, one should use a non-stationary scheme with a suitably small value of Δt.

Note that in the considered case of parallel isobaths, for the y-coordinate directed along the shoreline, it is sufficient to take $J = 3$, owing to the use of the "fluid" boundary conditions at the lines with $j = 1$ and $j = 3$ (see subsection 3.1 above for clarification). Such an approach is evidently equivalent to the case of the infinitely long shoreline, and evolution of the wave spectrum is one-dimensional. Herewith, this approach permits the solution of the problem with a minimum of PC resource.

4. RESULTS OF CALCULATIONS AND ANALYSIS

A representative set of model runs is presented in Table 1. The choice of runs is provided by the items of tasks named at the end of Section 2. Calculation results for the integral features of wave spectra in the most general form are presented in Table 2. Whilst the results are analysed, attention is paid to the frequency interval $\sigma \geq \sigma_p$, for which the applicability of the theoretical approach is accepted as proved, in accordance with verification of the model in Piscopia et al. (2003).

Table 1 Representative set of model runs.

Number of run	Parameters h_0, s and interval of $k_p h$	Angular parameter n	Shape parameter γ	Initial value A_p	Initial value B	Initial value θ_p, degrees
CONSTANT DEPTH SLOPE						
1	$h_0 = 10m$ $s = 0.05$; $2.36 > k_p h > 0.5$	2	1	0.64	0.68	0
2	$h_0 = 5m$ $s = 0.025$; $1.33 > k_p h > 0.35$	2	1	0.64	0.68	0
3	-"-	2	3	0.64	0.33	0
4	-"-	12	1	1.41	0.68	0
5	-"-	12	1	1.41	0.68	40
DEPTH PROFILE WITH A BAR						
6	Bar of form (16) $0.74 > k_p h > 0.5$	2	1	0.64	0.68	0
7	-"-	12	1	1.41	0.68	0
8	-"-	12	1	1.41	0.68	40

Table 2 Integral characteristics of calculated stationary two-dimensional spectra.

No. of run	$E(1) / E(10)$*		$A(\sigma_p) \mid_{i=10}$		B(10)*		$\theta_p(10)$ [grad] | $\sigma_p(10)$ [Hz]*	
	$c_{NL}=0$	$c_{NL}=1$	$c_{NL}=0$	$c_{NL}=1$	$c_{NL}=0$	$c_{NL}=1$	$c_{NL}=0$	$c_{NL}=1$
CONSTANT DEPTH SLOPE								
1	0.99	0.91	1.62	1.54	0.61	0.84	0 | 0.21	0 | 0.21
2	0.67	0.65	1.74	1.33	0.57	1.77	0 | 0.24	0 | 0.21
3	0.63	0.61	1.74	1.22	0.29	1.2	0 | 0.24	0 | 0.21
4	0.51	0.53	2.88	1.93	0.56	1.86	0 | 0.24	0 | 0.21
5	0.89	0.86	2.0	1.83	0.58	1.65	15 | 0.24	20 | 0.21
DEPTH PROFILE WITH A BAR								
	$E(1)/E(7) \mid E(10)/E(7)$*		$A(\sigma_p) \mid_{i=7} \mid A(\sigma_p) \mid_{i=10}$ $[A(\sigma_p(7)) \mid_{i=10}]$*		B(7) | B(10)*		$\sigma_p(7)$ [Hz] | $\sigma_p(10)$ [Hz]*	
	$c_{NL}=0$	$c_{NL}=1$	$c_{NL}=0$	$c_{NL}=1$	$c_{NL}=0$	$c_{NL}=1$	$c_{NL}=0$	$c_{NL}=1$
6	0.91 | 0.87	0.79 | 0.93	0.92 | 0.65	0.85 | 0.63	0.63 | 0.67	0.97 | 1.12	0.24 | 0.24	0.21 | 0.21
7	0.81 | 0.90	0.68 | 0.97	1.83 | 1.24	1.80 | 2.28 [1.21]	0.63 | 0.66	1.24 | 1.45	0.24 | 0.24	0.18 | 0.57
8	1.02 | 0.86	0.85 | 0.93	1.58 | 1.00	1.60 | 1.85 [1.00]	0.64 | 0.68	1.18 | 1.46	0.24 | 0.24	0.21 | 0.57

* Numbers in brackets denote the grid point indices along axes *OX*.

4.1 Constant slope case

4.1.1 Wave energy spatial distribution

For the visible estimation of the effect, the wave energy spatial distribution, $E(x)$, for linear and nonlinear cases is shown in Fig. 2. But the following qualitative discussion is based on the results presented in Table 2. In Table 2 the main energy distribution information is represented by the ratio of its initial value (i.e. energy at the point $i = 1$) to energy at the point nearest to the shore (i.e. the point with number $i = 10$).

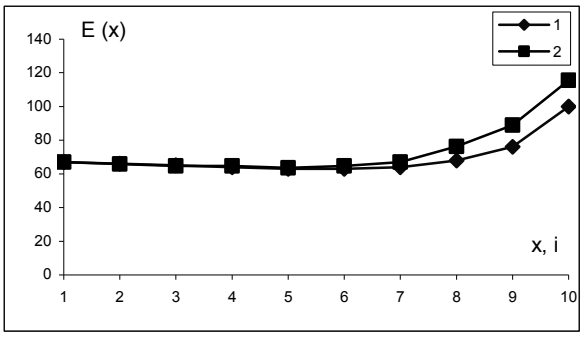

Fig. 2 Spatial distribution of wave energy $E(x)$ (run 2). 1 – linear case; 2 – nonlinear case (conventional units, in percentage of $E(10)$ for linear task).

From Table 2 it is seen that for run 1, when the minimal relative depth is $k_p h = 0.5$, the difference of energy for the linear and nonlinear cases is of the order of 10%. In other runs this difference is smaller (due to strong shoaling), but in the nonlinear case ($c_{NL} = 1$), the wave energy level near the shore is always higher.

In fact, diminishing $k_p h$ to the value 0.35 (runs 2–5) leads to equalling of all values $E(10)$ due to shoaling effect. This result testifies a smaller rate of the energy increase due to the nonlinearity with respect to one due to the shoaling, for the considered depth profile case. But there is a tendency in wave energy increase in the nonlinear case.

The following explains the effect of additional growth of wave energy in the nonlinear case, when wave propagation into the shallow water zone takes place. According to wave evolution Eq. (1) and ratio (2), the density of energy flux should be constant along the way. For this reason, as it is well known for the case $c_{NL} = 0$ (Polnikov and Sychev, 1996; Krasitskii, 1974), whilst diminishing values of $k_p h$, the wave energy begins to decrease due to a refractive narrowing of the angular spreading function of the wave spectrum, which leads to increasing mean wave speed. But further diminishing the depth (when $k_p h < 1$) leads to a wave energy growth, as the main part of the wave components is retarding (for details, see Krasitskii (1974)) [2].

For the nonlinear waves, the mean energy transport speed is diminishing additionally for the reason of increasing high-frequency (low speed) wave components portion in the wave spectrum, which is the main feature of the three-wave processes (see Fig. 3, and text in Polnikov, 2000). The one-dimensional spectra in both cases are shown in Fig. 4.

In accordance with these features of the non-linear process, the above gives the needed explanation of the additional energy growth due to nonlinearity. But for very small depths ($k_p h \le 0.5$), this additional effect is relatively small with respect to that of the shoaling, as it is seen from the presentation in Table 2.

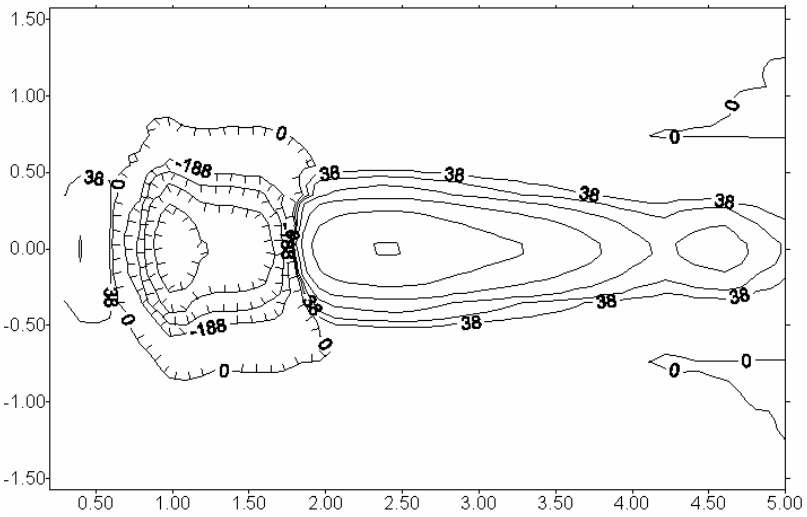

Fig. 3 Two-dimensional nonlinear transfer in the quasi-kinetic approximation (for the initial condition of run 3). Values of the transfer are given in conventional units as in Polnikov (2000). Negative values of the transfer are marked by hatches directed inside.

[2] This is the essence of the shoaling effect explanation.

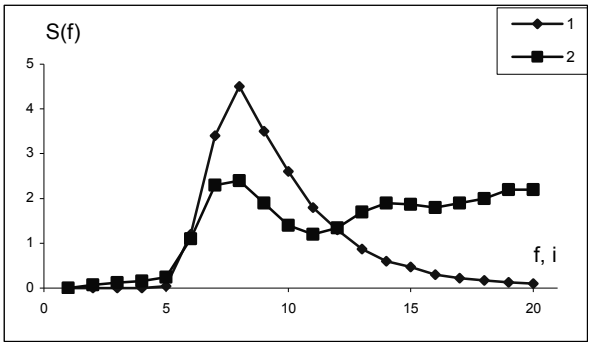

Fig. 4 One-dimensional spectrum shape at the 7th point near the shore (run 2): 1 – linear case, 2 – nonlinear case (conventional units).

4.1.2 Integral angular parameters distribution

Let us consider now a changeability of integral angular and frequency parameters of the two-dimensional spectrum, taking into analysis values of the angular narrowness at the peak frequency, $A_p = A(\sigma_p)$, and the frequency width, B, given by Eqs. (12)–(13). Numerical results for space distribution of $A_p(x)$ and $B(x)$ are given in Fig. 5.

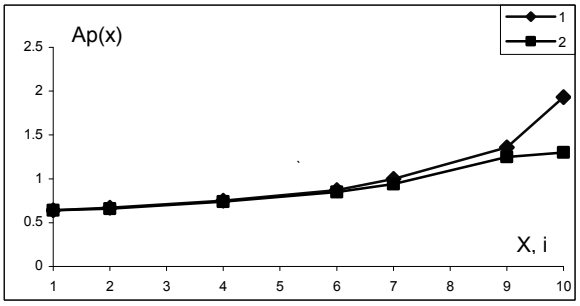

(a)

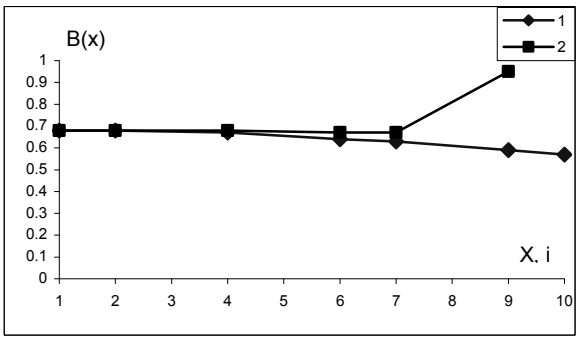

(b)

Fig. 5 Spatial distribution of integral parameters (run 2): a) $A_p(x)$, b) $B(x)$: 1 – linear case, 2 – nonlinear case.

As to the angular narrowness, the following is observed. Firstly, the angular narrowness value A_p is always significantly increasing, as it may be expected according to the refraction theory. Thus, the refractive effect of narrowing two-dimensional spectrum does always take place (see Table 2).

Secondly, in the nonlinear case, the narrowing effect is reasonably weaker: a relative weakening may reach 30% of the value of A_p found for the linear case (run 4). In other words, the nonlinearity counteracts the refractive narrowing of the wave spectrum. The extent of weakening of the refractive narrowing does increase with the relative depth and decrease (compare runs 1 and 2) with increasing wave slope (runs 2 and 3), and increasing initial narrowness of the spectrum (runs 2 and 4). The latter feature is due to the increasing intensity of the omni directed wave components, which leads to an increase in the intensity of nonlinear interactions among waves. This effect is more evidently seen from the distribution of $A(\sigma)$ at the final point (Fig. 6).

An explanation of the weakening effect on the spectrum narrowing due to refraction is related to the structure of the nonlinear energy transfer in the three-wave approximation (Fig. 3). According to Polnikov (2000), the energy is transferred from the spectral peak domain (near the frequency σ_p) to the higher frequency domain where $\sigma \geq 2\sigma_p$. Thus, all the mentioned features of the weakening of the spectrum angular narrowing are wholly explained by the strengthening of the nonlinear interactions.

Thirdly, for waves with general direction θ_p to the normal of the shore, the spectral narrowing effect and effect of its weakening are reasonably less expressed (compare runs 4 and 5 in Table 2). The strength of such an effect evidently depends on the initial value of θ_p.

An explanation of the latter effect (taking place both in linear and nonlinear cases) consists in the following feature of refraction. In the case when θ_p is not normal to the shore, some wave components (which are closer to the normal) deviate stronger from the initial direction than θ_p does, but other components (which are farther from the normal than θ_p) cannot follow the change of the value of $\theta_p(x)$. As a result, the pure refractive narrowing of the spectrum becomes weaker. Eventually, this effect leads to a weakening of the nonlinear transfer intensity, as it was explained above when the features of nonlinear processes are discussed.

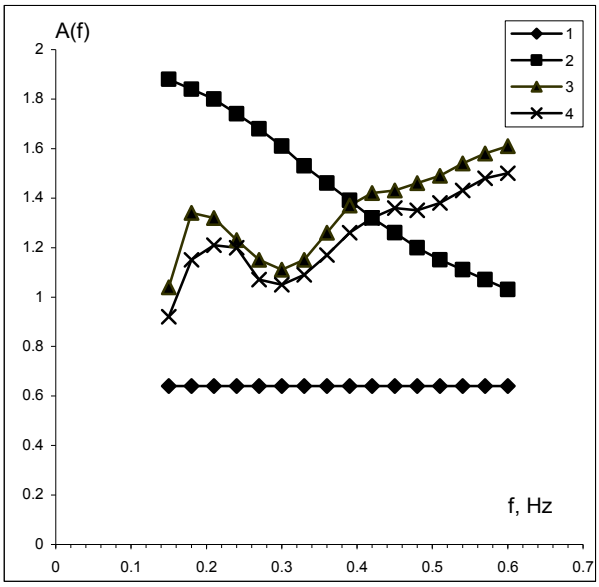

Fig. 6 Dependence of the angular narrowness on frequency, $A(f)$, at the point i=10:
1 – initial angular narrowness function for runs 2 and 3
2 – angular narrowness function for a stationary solution of linear case for runs 2 and 3
3 – angular narrowness function for a stationary solution of nonlinear case for run 2
4 – angular narrowness function for a stationary solution of nonlinear case for run 3
Initial peak frequency f_p=0.24 Hz.

It is worth mentioning especially the effect of increase in the spectrum narrowness with the increase in frequency, which is due to the peculiarity of the three-wave interactions as well (Fig. 6). From this figure it is seen that for the nonlinear waves, in contrast to the case when $c_{NL}=0$, the value of $A(\sigma)$ at frequencies $\sigma \geq 2\sigma_p$ may reach magnitudes in $1,2$ times greater than $A(\sigma_p)$. This effect was not mentioned in the literature before. Its main feature is a substantial difference of high-frequency narrowness of wave spectrum in linear and nonlinear cases. One should expect that wave breaking will not reasonably change the strength of the effect discussed, as far as all known formulations of the term *BR* for shallow water are linear in the spectrum (Battjes and Janssen, 1978; Piscopia et al., 2003). The latter means that the term *BR* influences weakly on the angular spreading. Maybe just for this reason, the turning of waves is well seen visually near the shore despite the nonlinear weakening of the spectrum turning in the peak frequency domain (run 5).

4.1.3 Integral frequency parameters distribution

About the spatial distribution of the frequency width of the spectrum, $B(x)$, one may draw the following conclusions.

Firstly, in the linear case, the shoaling effect leads to small, though remarkable (of the order of 10%), decrease of the magnitude B. In the nonlinear case, on the contrary, a substantial increase (3–4 times) in the spectral frequency width is noted. On the other hand, a strong counteraction of the nonlinearity to the shoaling takes place. This effect was also revealed earlier in Polnikov (1998) and Piscopia et al. (2003). But here we have found additionally that the nonlinearity impact on the spectral shape formation is enhancing whilst the narrowness of initial angular function of the spectrum increases (compare runs 2 and 4 in Table 2). Evidently, this effect is due to the intensification of the nonlinearity itself.

Secondly, the mentioned effect of the frequency spectrum widening is enhancing with the depth decreasing and wave slope increasing (due to the increases in nonlinearity, in this case, evidenced from formulas (5) and (9)). But the effect becomes weaker whilst the initial general direction of waves deviates form the normal to the shore (Table 2).

The nature of these features of spectrum widening is the same as the one mentioned when the angular effects are explained above. In all cases mentioned, just the angular distribution of wave energy in the spectrum governs the intensity of nonlinear interactions and results in the effects discussed.

4.1.4 Spatial distribution of θ_p and σ_p

A character of the spatial distribution of the general wave direction, θ_p, and the spectral peak frequency σ_p may be analyzed by their limiting values at the grid point nearest to the shore. Without details, here we should note the following.

Taking into account the results for run 5, it is seen that the nonlinearity makes weaker the rate of variation of $\theta_p(x)$ due to refraction. This effect is explained by the fact of energy transfer from the spectral peak domain to higher frequencies, changing the frequency-angular structure of the spectrum in whole (Fig. 3). As seen, this process has an influence on the distribution of $\theta_p(x)$.

In the case of rather strong nonlinearity (all runs except the first one), a decrease of the spectral peak frequency value $\sigma_p(10)$ when $c_{NL}=0$ is observed. This effect, evidently, is due to the fact

of nonlinear energy transfer from the spectral peak domain to higher frequencies, resulting in a shift of the main peak to the lower frequencies (see also Piscopia et al., 2003).

4.2 The depth profile with a bar

Consider now calculation results for the case of depth profile with a submerged bar described by Eq. (16), comparing them to results for the constant slope depth. Herewith, the point with index $i = 7$ should be taken as the additional control as the depth at this point starts to grow. For this reason, the relative values of the wave spectrum parameters are of interest at the initial, intermediate ($i = 7$), and final grid points. Some results are plotted in Fig. 7. Generalized presentation is given in Table 2.

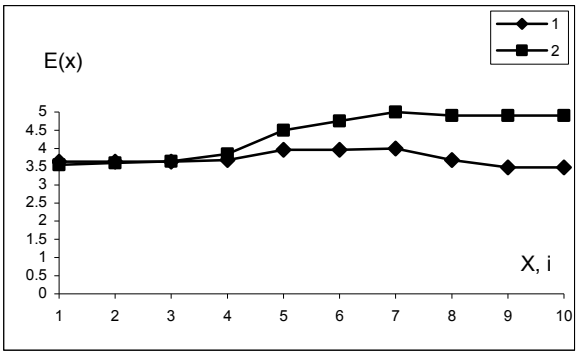

(a)

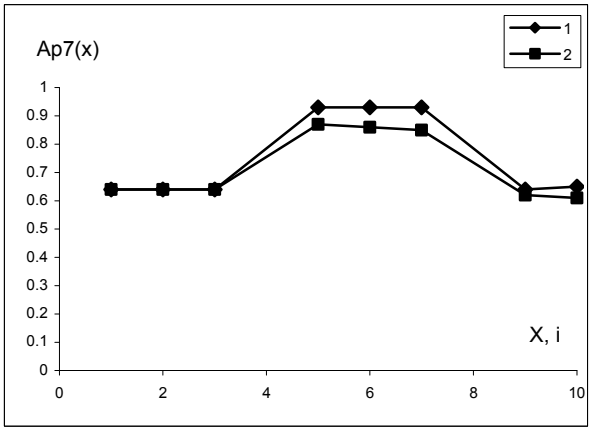

(b)

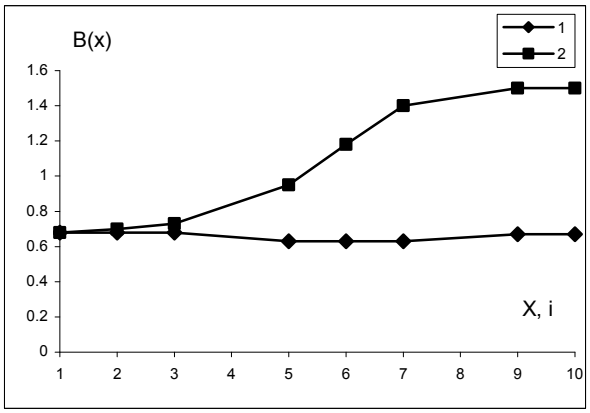

(c)

Fig. 7 Spatial distribution of integral parameters in the case of bar profile: a) $E(x)$, b) $A_p(x)$, c) $B(x)$: 1 – linear case, 2 – nonlinear case.

4.2.1 Wave energy distribution

Firstly, as seen in the second part of Table 2, in the nonlinear case, a high energy level is maintained with respect to the linear case, in addition to the above mentioned effect of energy enhancing at the point of maximal refraction ($i = 7$). Note that in the linear case, the wave energy is damped due to an "inverse shoaling" effect whilst the depth becomes greater. The difference between energy levels, in these two cases, is not too great, but it may reach up to 10–20% (run 7).

As explained in subsection 4.1.2, it is clear that the effect described is more remarkable for a narrower angular distribution of the initial spectrum (compare runs 6 and 7), as the nonlinear interaction intensity is greater in such a case.

Secondly, for the initial general direction θ_p from the normal to the shore, the effect is weaker. Explanation of this effect is the same as in subsection 4.1.2.

In the nonlinear case, a reason for a high wave energy level maintained after transition through a submerged bar domain is that the nonlinear interactions are continuing to act intensively because water is still shallow, and a reasonable part of the energy is located at high frequencies. Therefore, an intensive transfer of energy continues into the high frequency domain where the "inverse shoaling" does not work.

4.2.2 Integral frequency and angular parameters distribution

In the bar case, it is interesting to note the process describing a return of the angular narrowness value A_p to its initial one. It is seen in Table 2 that if a jump of peak frequency to the upper limit of the frequency interval is not realized (this effect is

discussed below) in the nonlinear case, the said return takes place with a surplus (i.e. $A_p(10)$ is even lower that $A_p(1)$). The reason for the effect is the same: an intensive transfer of energy from the peak frequency domain to the upper frequencies along the whole wave trajectory, both before and after the bar.

In addition, it is important to note that in the case of a peak frequency jump to the upper frequencies, a sharp increase in the angular narrowness $A_p(10)$ is observed at the new peak frequency (runs 7 and 8). This specific effect of the angular narrowing at high frequencies due to the nonlinearity was already discussed above. But in this case, it is manifested much stronger.

Regarding the spectrum frequency width one can note that in the linear case, the final value, $B(10)$, equals to the initial one, $B(1)$ (Fig. 7c). But in the nonlinear case, remarkable frequency widening is observed at the point $i = 7$, followed by a subsequent growth of B after passing the bar. It is interesting that for the depth profile with a bar, a change of initial general direction θ_p does not influence the values of B at the control points after passing the bar. Apparently it is explained by an accidental combination of depths and distances in the profile chosen. In principle, a nonlinear influence must be weaker with an increase in initial deviation of θ_p from the normal to the shore (or to the bar) for the reason mentioned in subsection 4.1.2.

4.2.3 Distribution of θ_p and σ_p

As regards the general wave direction distribution, $\theta_p(x)$, no peculiarities were revealed in all runs. For instance, in run 8, the distribution $\theta_p(x)$ is the same for both linear and nonlinear cases and similar to the case of constant depth slope. For this reason it is not presented in Table 2.

The spectrum peak frequency distribution, $\sigma_p(x)$, has peculiarities depending on the spectrum shape and value of the nonlinearity parameter, c_{NL}. As seen from Table 2, in the linear case, the value $\sigma_p(x)$ does not vary. In the nonlinear case, both a decrease of σ_p (runs 6 to 8, point $i = 7$) and a jump of σ_p to the upper limit of the frequency interval used for calculations (runs 7 and 8, point $i = 10$) are observed.

Firstly, note that the difference between the runs is due to a different extent of the nonlinear interaction intensity, which in turn is due to the difference of the initial spectrum shapes. It is clear that the nonlinear interactions become stronger with an increase in the angular narrowness (whilst other spectrum parameters are the same) due to a greater density of the wave energy in the (σ, θ)-space. Remember that analogous effect also takes place in the constant depth slope case.

Secondly, a strengthening of nonlinearity results in a quicker transfer of energy to higher frequencies, which provides a jump of the spectrum peak to the upper limit of the frequency interval. This effect, as mentioned in Polnikov (1998) and numerically proved in Piscopia et al. (2003), is not realized in practice for the reason of intensive wave breaking at high frequencies. But, here, the local secondary peaks of the spectrum at frequencies multiple of σ_p remain (see figures in Piscopia et al., 2003). Due to this circumstance we put especially in Table 2 (in square brackets) the angular narrowness parameter at the real peak frequency, $\sigma_p(7)$.

The one-dimensional and two-dimensional spectrum shapes are given in referenced papers and are not repeated here.

5. TESTING SWAN MODEL

All previous features of nonlinearity in shallow water are rather important from a physical point of view. Thus they should all be reproduced in any sophisticated practical model. One of such model is the *SWAN* one, which is widely used in practical calculations. Thus, it is worthwhile to check the properties of the *SWAN* nonlinear term with respect to the results obtained before. But in this checking one should switch off any dissipation terms making it similar to our test senarios. Test results are presented in Figs. 8, 9 and 10. All features of numerics can be found in the SWAN User Manual (2004).

It needs to mention that here we show only a part of the numerical results obtained with *SWAN*, related just to the non-stationary mode as results for the stationary mode are less treatable and will be discussed in a separate paper in future.

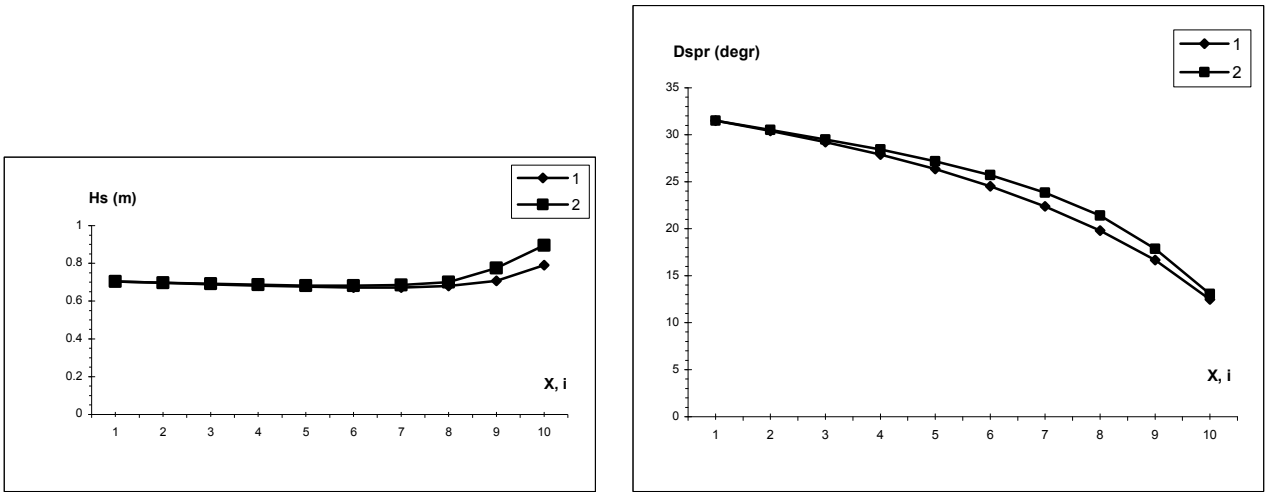

(a) (b)

Fig. 8 Spatial distribution of integral parameters in the SWAN model for constant slope case: a) $H_S(x)$, b) $DSPR(x)$: 1 – linear case, 2 – nonlinear case.

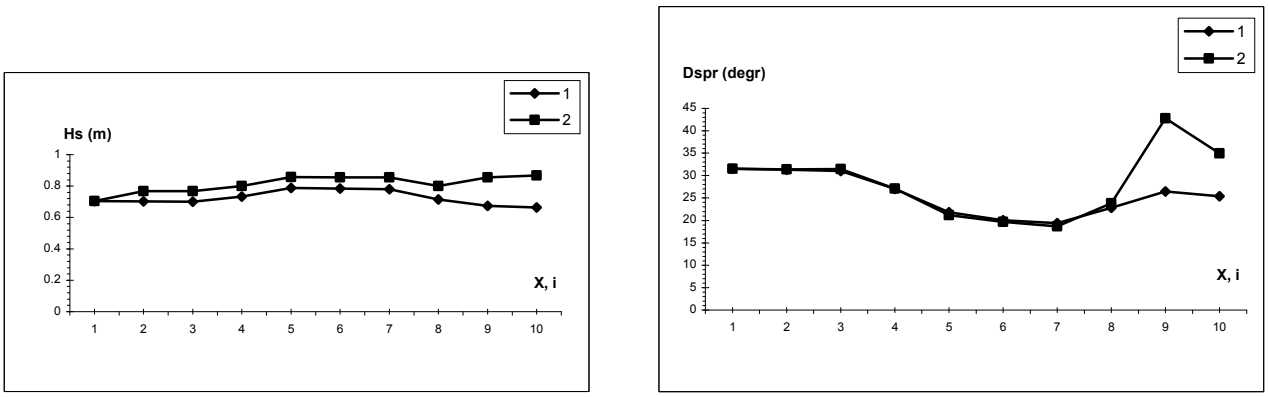

(a) (b)

Fig. 9 Spatial distribution of integral parameters in the SWAN model for bar case: a) $H_S(x)$, b) $DSPR(x)$: 1 – linear case, 2 – nonlinear case.

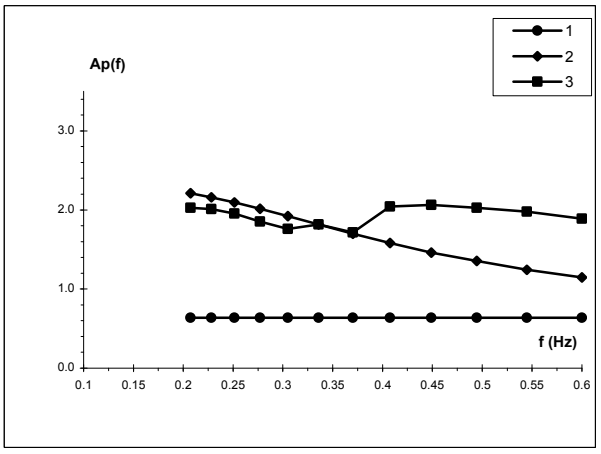

Fig. 10 Dependence of the angular narrowness on frequency, $A(f)$, in the SWAN model at the point i=10 (run 2). 1 – initial value; 2 – linear case; 3 – nonlinear case.

From Figs. 8 and 9 one can see very similar behaviour of integral characteristics (significant wave height, $H_S(x)$, and angular dispersion, $DSPR(x)$[3]) as functions of space in both cases of depth profile. The only remarkable difference is seen for energy distribution at the initial points. We consider this as the property of the numerical scheme used in *SWAN*. But, in principle, energy enhancement at the final point and after bar crossing is conserved by the *SWAN* model in accordance with the exact numerical solutions obtained above.

But from Figs. 8 and 9 the counteraction of nonlinearity to refraction is not evidently seen. To this aim, we plot additionally Fig. 10 as we did for Fig. 6 for frequency distribution of angular narrowness function at the final point $i = 10$ for

[3] For definition, see SWAN User Manual (2004).

run 2. Fig. 10 demonstrates very similar behaviour of $A_p(f)$ for the nonlinear case, that is, we can evidently see the work of nonlinearity against refraction. In the *SWAN* model nonlinearity makes refraction narrowing weaker at lower frequencies, and at higher frequencies it makes narrowing stronger, in full accordance with the exact theoretical results shown before. Thus, we may state that the *SWAN* model reveals principally the main properties of the exact nonlinear model in the frame of three-wave quasi-kinetic theory.

Of course, the extent of representation of features on nonlinearity in the *SWAN* model is not absolute. In this study we did not vary some options in *SWAN* nonlinear parameterization codes to reach better results. In any case, this aim could be reached by making a proper correction of the parameterization of the three-wave nonlinear term used in *SWAN*. Mainly it related to the intensity coefficient of the parameterization in Eldeberky and Battjes (1996). But this is a task for detailed investigations in future.

6. CONCLUSIONS

On the basis of the results obtained we can draw the following conclusions.

1. The relative roles of the depth refraction and three-wave nonlinearity are fairly different for different spectrum characteristics. The depth refraction and three-wave nonlinearity are equally substantial in their influence on the variation of the angular features of two-dimensional spectra. At the same time, the frequency shape of the two-dimensional spectrum is almost completely controlled by the nonlinear processes.
2. The nonlinearity counteracts the refractive change of the angular features of the wave spectrum. At the peak frequency the nonlinearity diminishes the angular narrowness parameter by 10–30%, but at the higher frequencies, in contrast, it increases the latter by 2–3 times.
3. It is numerically established that the refraction process leads to an additional increase in nonlinearity intensity. This effect is due to the dependence of nonlinear interactions intensity on the extent of angular spreading of wave energy, i.e. on the angular narrowness of spectrum.[4]

As a whole, one may conclude that the shallow water refraction and the nonlinearity are equally important for calculations of wave characteristics in shallow water. Accounting for the nonlinearity is very important in describing shape changes in both one-dimensional and two-dimensional spectra. But the refraction is naturally accounted for in the latter case only. Here, accounting for the refraction permits simultaneously more accurate estimation of the nonlinearity impact on evolution of two-dimensional spectrum shape.

At present, the *SWAN* model demonstrates the main properties of the nonlinearity revealed from the exact three-wave quasi-kinetic theory. Thus, one may expect that the *SWAN* software gives reasonable results of numerical calculations of nonlinear waves. But we should mention that in the nonlinear case one should use the non-stationary mode of the model.

ACKNOWLEDGEMENTS

The authors are grateful to Mr. M. Zaslavskii for stimulating interest in the work and discussion of results at the preliminary stage. This work was supported by the science fellowship fund of the University of Rome “La Sapienza” and the Russian Foundation for Basic Research, project # 01-05-64580. The authors are thankful to Prof. A. Noli and Dr. A. Panizzo for helping to organize work at the University and interest in the work.

REFERENCES

1. Battjes JA, Janssen JPFM (1978). Energy Loss and Set-up due to Breaking of Random Waves. *Proc. 16th Int. Conf. on Coastal Eng.* pp. 569–587.
2. Beji S, Battjes JA (1993). Experimental Investigation of Wave Propagation over a Bar. *Coastal Eng*. 19:151–162.
3. Eldeberky Y (1996). *Nonlinear Transformation of Wave Spectra in the Nearshore Zone*. Ph.D. thesis. Delft University of Technology. 204 p.
4. Eldeberky Y, Battjes JA (1996). Spectral Modeling of Wave Breaking: Application to

[4] Noted in Henderson et al. (2006) that the authors seem to have registered an experimental evidence of the effect under our consideration. More experimental information is needed for verifying this assumption, which could be done in a separate paper later.

Boussinesq Equation. *J. Geophys. Res.*, 101C, 1253–1264.
5. Freilich MH, Elgar GL, Guza RT (1990). Observations of Nonlinear Effects in Directional Spectra of Shoaling Surface Gravity Waves. *J. Geophys. Res.*, 95C, 9645–9656.
6. Hasselmann K, Ross DB, Muller P, Sell W (1976). A Parametric Wave Prediction Model. *J. Phys. Oceanogr*. 6:200–228.
7. Henderson SM, Guza RT, Elgar S, Herbers THC (2006). Refraction of Surface Gravity Waves by Shear Waves. *J. Phys. Oceanogr*. 36(4):629–635.
8. Kitaigorodskii SA, Krasitskii VP, Zaslavskii MM (1975). On Phillips' Theory of Equilibrium Range in the Spectra of Wind-generated Gravity Waves. *J. Phys. Oceanogr.* 5:410–420.
9. Krasitskii VP (1974). To the Theory of Spectrum Transformation During Wind Waves Refraction. *Izv. Acad. Nauk, Fiz. Atmos. Okeana* 10:72–82 (in Russian).
10. Piscopia R, Polnikov VG, de Girolamo P, Magnaldi S (2003). Validation of the Three-Wave Quasi-Kinetic Approximation for the Spectral Evolution in Shallow Water. *Ocean Engineering* 30:579–599.
11. Polnikov VG (1998). Studying the Equations of the Three-Wave Quasi-Kinetic Approximation for Nonlinear Gravity Waves in a Finite-Depth Water. *Izv. Atmos. Okean. Phys.* 34:757–764 (English transl.).
12. Polnikov VG (2000). Two-Dimensional Nonlinear Energy Transfer over the Spectrum of Waves in a Finite-Depth Water in the Three-Wave Quasi-Kinetic Approximation. *Izv. Atmos. Okean. Phys.* 36:651–660 (English transl.).
13. Polnikov VG, Sychev EN (1996). Numerical Modelling of Wave Spectrum Evolution for Shallow Waters. *Okeanologiya* 36:779–786 (English transl.).
14. Smith Mckee J (Ed) (2004). *Proceedings of 29th International Conference of Coastal Engineering*. World Scientific, USA, 1, 1118.
15. SWAN User Manual (2004). SWAN Cycle III, version 40.41, Delft University of Technology. 135 p.
16. Zakharov VE (1998). Weakly Nonlinear Waves on the Surface of an Ideal Finite Depth Fluid. *Amer. Math. Soc. Transl.* 182:167–197.
17. Zaslavskii MM, Krasitskii VP, Gavrilin BL (1995). Shallow Water Limitations for Application of the Four-Wave Interactions of Nonlinear Waves in the Finite Depth Water. *Proc. of Conference on Dynamics of Ocean and Atmosphere*. Moscow. p. 139.
18. Zaslavskii MM, Polnikov VG (1998). Three-Wave Quasi-Kinetic Approximation in the Problem of the Evolution of a Spectrum of Nonlinear Gravity Waves at Small Depths. *Izv. Atmos. Okean. Phys.* 34(5):609–616 (English transl.).
19. Young IR, Verhagen LA, Khatri SK (1996). The Growth of Fetch Limited Waves in Water of Finite Depth. Pt. 3. Directional Spectra. *Coastal Engineering* 29:101–121.